

Infant movement classification through pressure distribution analysis – added value for research and clinical implementation

Tomas Kulvicius^{1,2*~}, Dajie Zhang^{1,3,4*}, Karin Nielsen-Saines⁵, Sven Bölte^{6,7,8}, Marc Kraft⁹, Christa Einspieler⁴, Luise Poustka^{1,3}, Florentin Wörgötter^{3,9+}, Peter B Marschik^{1,3,4,6+}

1. Child and Adolescent Psychiatry and Psychotherapy, University Medical Center Göttingen, Göttingen, Germany
2. Department for Computational Neuroscience, Third Institute of Physics-Biophysics, Georg-August-University of Göttingen, Göttingen, Germany
3. Leibniz-ScienceCampus Primate Cognition, Göttingen, Germany
4. iDN – interdisciplinary Developmental Neuroscience, Division of Phoniatics, Medical University of Graz, Graz, Austria
5. Division of Pediatric Infectious Diseases, David Geffen UCLA School of Medicine, Los Angeles, USA
6. Center of Neurodevelopmental Disorders (KIND), Centre for Psychiatry Research; Department of Women’s and Children’s Health, Karolinska Institutet, Stockholm, Sweden
7. Child and Adolescent Psychiatry, Stockholm Health Care Services, Region Stockholm, Stockholm, Sweden
8. Curtin Autism Research Group, Curtin School of Allied Health, Curtin University, Perth, Western Australia
9. Department of Medical Engineering, Technical University Berlin, Berlin, Germany

~Corresponding author (E-mail: tomas.kulvicius@uni-goettingen.de)

*These authors share first authorship

+These authors share senior authorship

ABSTRACT

In recent years, numerous automated approaches complementing the human Prechtl’s general movements assessment (GMA) were developed. Most approaches utilised RGB or RGB-D cameras to obtain motion data, while a few employed accelerometers or inertial measurement units. In this paper, within a prospective longitudinal infant cohort study applying a multimodal approach for movement tracking and analyses, we examined for the first time the performance of pressure sensors for classifying an infant general movements pattern, the fidgety movements. We developed an algorithm to encode movements with pressure data from a 32x32 grid mat with 1024 sensors. Multiple neural network architectures were investigated to distinguish *presence* vs. *absence* of the fidgety movements, including the feed-forward networks (FFNs) with manually defined statistical features and the convolutional neural networks (CNNs) with learned features. The CNN with multiple convolutional layers and learned features outperformed the FFN with manually defined statistical features, with classification accuracy of 81.4% and 75.6%, respectively. We compared the pros and cons of the pressure sensing approach to the video-based and inertial motion sensor-based approaches for analysing infant movements. The non-intrusive, extremely easy-to-use pressure sensing approach has great potential for efficient large-scaled movement data acquisition across sites and for application in busy daily clinical routines for evaluating infant neuromotor functions. The pressure sensors can be combined with other sensor modalities to enhance infant movement analyses in research and practice, as proposed in our multimodal sensor fusion model.

1. INTRODUCTION

In the past decades, knowledge on human spontaneous movements, their onset, developmental trajectory, and predictive significance for developmental outcomes was profoundly advanced [1]. Among the rich repertoire of human spontaneous movements, the clinical value of a specific motor pattern, termed general movements by Prechtl and colleagues [2, 3], has gained substantial clinical attention. General movements originate by 8 to 10 weeks' gestation and involve the entire body [4]. These motor patterns present astonishing continuity from the foetal period to the first few weeks after birth, yet transform dramatically in appearance during the second to the third month of life. This coincides with the well-known three-month transformation, where infants manifest significant changes across developmental domains (e.g., movements, vision, vocalisation, social-cognition; [5]). The method of choice [6] to assess early spontaneous movements and their transformation is a non-intrusive Gestalt-based observational method, the Prechtl's general movement assessment (GMA). Ever since its establishment, the GMA has repeatedly proven its value in distinguishing different movement patterns which predict distinctive outcomes. Intensive research has documented the normal patterns and their developmental trajectories from foetal general movements to the onset of voluntary motor functions [1, 4]. Studies into the potential pathology associated with general movements identified a range of aberrant movement patterns in young infants with brain lesions, various genetic disorders, autism spectrum disorder, and alterations induced by antenatal infectious exposures such as arboviruses and other pathogens or following a range of antenatal viral infections which can deleteriously affect the central nervous system (for a review see [7]). The significance of general movements in early brain development and, consequentially, its long-term relevance for cognitive, speech-language, and motor development has long been recognised [8, 9, 10, 11, 12].

General movements are triggered by the central pattern generators (CPGs; [13]). Variability in the motor output is achieved by supraspinal projection, inhibition, and, most importantly, modulation of CPG activity. If the CPGs exhibit reduced modulation, less variable, i.e., abnormal, movements will present, indicating foetal or neonatal compromise [4]. Before term age, GMs are referred to as foetal or preterm GMs, whereas movements observed between term age and approximately 6–8 weeks of post-term age are termed writhing movements (WMs; [4]). Normal writhing movements are variable sequences of neck, trunk, leg, and arm movements, with gradual initiation and termination and of changing intensity, force, and speed. Spontaneous writhing movements can last between seconds and several minutes. During the writhing movements period, abnormal patterns include *poor repertoire*, *cramped-synchronised*, or the very rare *chaotic* patterns. Writhing movements gradually disappear during the second to third month of post-term age, and a new pattern of general movements, the fidgety movements (FM), sets in. Normal fidgety movements are small amplitude movements of moderate speed with variable acceleration of the neck, trunk, and limbs in all directions. They are continuously observable during active wakefulness. A disruption in the developing nervous system will manifest itself by aberrant, or an *absence* of, fidgety movements. The absence of FMs at 3–5 months of post-term age is a sensitive and specific predictor for neurological impairment (e.g., cerebral palsy; [14]), which has received great attention in research and clinical fields. Fidgety movements gradually fade out by 20 weeks of post-term age when voluntary movement patterns become predominant [4, 10].

Augmenting the classic GMA, increasing efforts on automated solutions to classify infant motor functions have taken place. While most attempts have been, inherent to the GMA methodology and focused on video-based solutions, we launched in the past decade a multimodal approach to study infant neurodevelopmental functions utilising, in addition to a multi-camera video set-up, inertial motion units (IMU, accelerometer data) and pressure sensing devices to analyse and quantify infant movements [5]. Different labs have followed the path and implemented methods using different sensors in their assessment of infant movements (for reviews see [15, 7]).

Most automated systems for infant movement assessment are based on video data captured by 2D RGB cameras [16, 17, 18, 19, 20, 21, 22, 23, 24, 25, 26, 27, 28, 29, 30, 31, 32, 33, 34, 35], RGB-D sensors

[36, 37, 38, 39, 40, 41, 42] or a multi-camera marker-based setup [43]. Some studies applied wearable sensors such as 3 DoF accelerometer sensors [44, 45], 6 DoF inertial motion unit (IMU) sensors [46, 47, 48], or an electromagnetic position tracking system [49, 50]. While external visual sensors and “on-body” wearable sensors have their pros and cons (see Discussion for comparisons), to the best of our knowledge, no study has yet utilised a pressure sensing mat to analyse infant motor patterns.

The application of pressure sensing mats as proposed in our novel approach [5] to model and predict infant motor development requires a feasibility verification. In current study, we used a pressure sensing mat for movement classification distinguish *presence* vs. *absence* of fidgety movements according to GMA. With a longitudinal prospective infant cohort, fortnightly collected movement data of each infant from 4 to 16 weeks of post-term age were analysed.

2. METHODS

2.1 Dataset

Data from a prospective longitudinal cohort of 51 typically developing infants were analysed [5, 31, 51]. Data acquisition was conducted at iDN’s BRAINtegrity lab at the Medical University of Graz, Austria, within an umbrella study profiling typical cross-domain development during the first months of life. Details on data recording and participant information have been previously described [31, 51]. Movement data were collected in form of RGB and RGB-D video streams, accelerometer and gyroscope data, plus pressure sensing mat data were all collected in a standard laboratory setting following Prechtl general movements assessment guidelines [4].

Pressure data was acquired using a Conformat pressure sensing mat (Tekscan, Inc., South Boston, Massachusetts, USA, [52]). This mat contains 1024 pressure sensors arranged in a 32 x 32 array on an area of 471.4 x 471.4 mm², producing pressure image frames (8 Bit, 32 x 32 pixels, sampling rate 100 Hz). The mat was laid beneath the cotton sheet of the cot mattress.

For the machine learning method, we segmented the data stream into 5-second snippets (for procedure and the rationale of the method, please see [31]). From a total of 19451 available snippets, 2800 were randomly selected for the current analyses. Data processing was performed at the *Systemic Ethology and Developmental Science Unit (SEE)*, Department of Child and Adolescent Psychiatry and Psychotherapy at the University Medical Center Göttingen, Germany. The GMA for the dataset was performed by two senior assessors (DZ, PBM; for details on the rating procedure please refer to [31]). The study was approved by the Institutional Review Board of the Medical University of Graz, Austria (27-476ex14/15) and the University Medical Center Göttingen, Germany (20/9/19). Parents were informed of all experimental procedures and study purpose, and provided their written informed consent for participation and publication of results.

2.2 Feature Extraction for Motion Encoding

A flow diagram of feature extraction procedure is shown in Fig. 1. As input, we use the 5s long recordings (corresponding to the 5s video snippets in a previous study with the same dataset [31]) with a sampling rate of 100 Hz. This rate was obtained from the pressure mat, which leads to 500 frames where one frame consists of 1024 pressure sensor values arranged on a 32x32 grid (32x32 pressure sensor values; see frames on the left side).

We first cropped the area [1:29, 4:29] of original grid size 32x32 (red rectangle) since in most of the cases the sensor values outside this area were 0, thus, the size of the cropped area was 29x26 leading to 754 pressure sensor values. In most cases only two areas were strongly activated on the pressure mat (see two examples in Fig. 3) where activations on the top correspond to infant shoulders and/or head and activations at the bottom correspond to infant hips. Therefore, we split the cropped grid of size 29x26 into two parts 12x26 (top) and 17x26 (bottom) and tracked the centre of mass of pressure in these two areas.

Next, we computed position coordinates x and y of the pressure mass centre and average pressure values p of the top and the bottom part for each frame as follows:

$$x_{t/b} = \frac{\sum_i i \times p_{t/b}(i,j)}{\sum_{i,j} p_{t/b}(i,j)}, \quad y_{t/b} = \frac{\sum_j j \times p_{t/b}(i,j)}{\sum_{i,j} p_{t/b}(i,j)}, \quad p_{t/b} = \frac{\sum_{i,j} p_{t/b}(i,j)}{m_{t/b} \times n_{t/b}}.$$

Here $p_t(i,j)$ and $p_b(i,j)$ correspond to pressure sensor values at the position ($i=1..m_{t/b}$, $j=1..n_{t/b}$) of the top (t) and bottom (b) parts, respectively. To reduce signal noise, for each value x , y , and p , we applied moving average filter with a sliding window of size 5 frames (0.05 s).

To avoid bias of the size and weight of the infant, we normalised values x , y , and p between 0 and 1 as follows:

$$x_{t/b} = \frac{x_{t/b} - \min(x_{t/b})}{\max[\max(x_t) - \min(x_t), \max(x_b) - \min(x_b), \max(y_t) - \min(y_t), \max(y_b) - \min(y_b)]},$$

$$y_{t/b} = \frac{y_{t/b} - \min(y_{t/b})}{\max[\max(x_t) - \min(x_t), \max(x_b) - \min(x_b), \max(y_t) - \min(y_t), \max(y_b) - \min(y_b)]},$$

$$p_{t/b} = \frac{p_{t/b} - \min(p_{t/b})}{\max[\max(p_t) - \min(p_t), \max(p_b) - \min(p_b)]}.$$

Thus, the original input of size $500 \times 32 \times 32$ is reduced to 500×6 , i.e., six signals of length 500 frames.

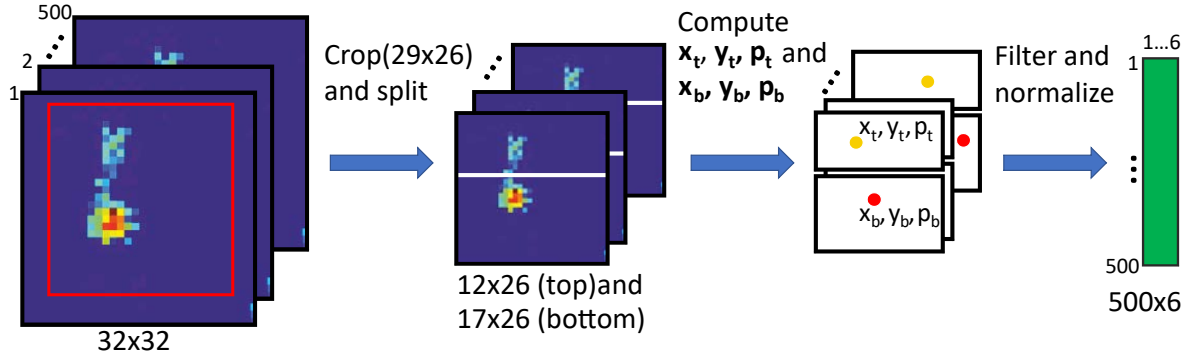


Figure 1: Flow diagram of the feature extraction procedure for the motion encoding.

2.3 Network Architectures

For classification of fidgety movements, we compared two neural network architectures, namely, a feed-forward network (FFN) architecture with manually defined features and a convolutional neural network (CNN) with learned features (for examples of network architectures see Fig. 2).

In case of the FFN we used statistical features obtained from signals $x_{t/b}$, $y_{t/b}$, and $p_{t/b}$ and their derivatives $x'_{t/b}$, $y'_{t/b}$, and $p'_{t/b}$ by computing mean and standard deviation values for each signal. In one case we only used statistical features from the original signals, which resulted into 12 input values in total, and in the other case we used statistical features from both original signals and their derivatives. This resulted into 24 input values in total. As shown in Table 1, we investigated FFN architectures with one fully connected (FC) layer with 12 or 24 inputs and with two fully connected layers.

In case of the CNN we used the original signals $x_{t/b}$, $y_{t/b}$, and $p_{t/b}$ as inputs and allowed the network extract features from these signals by utilising one or multiple convolutional layers. Behind the convolutional layer(s) we used an average pooling layer to reduce the input dimension as commonly used in convolutional network architectures. This was then followed by one or two FC layers. All details of the network architectures and their parameters can be found in Table 1 and schematic diagrams of one FFN architecture (F2) and one CNN architecture (C3F2) are presented in Fig. 2(a) and Fig. 2(b), respectively.

Network architectures were implemented using TensorFlow [53] and Keras API [54]. To train the network architectures we used the Adam optimiser with a binary cross-entropy as a loss function,

batch size 32, and default training parameters, i.e., learning rate = 0.001, $b_1 = 0.9$, $\beta_2 = 0.999$, and $e = 1e-07$. To avoid overfitting, we used validation stop with validation split 1/6 and patience 10.

Table 1: Details of the Feed Forward Network (FFN) and the Convolutional Neural Network (CNN) architectures. After each fully connected (FC) and convolutional layer (Conv) a batch normalisation layer and a drop-out layer (10%) were used. ReLU activation functions were used in FC and Conv layers, whereas in the output layer a sigmoid activation function was used.

| FFN | | | | | | | | |
|--------------------------------|------------|-----------------------|-----------------------|-----------------------|-----------------|--------------|--------------|-------------|
| Name | Input dim. | FC 1 neurons | FC 2 neurons | Output dimension | | | | |
| F1.1 | 12 | 100 | - | 1 | | | | |
| F1.2 | 24 | 100 | - | 1 | | | | |
| F1.3 | 24 | 200 | - | 1 | | | | |
| F2 | 24 | 200 | 100 | 1 | | | | |
| CNN with one conv. layer | | | | | | | | |
| Name | Input dim. | Conv 1 filters / size | Conv 2 filters / size | Conv 3 filters / size | Average pooling | FC 1 neurons | FC 2 neurons | Output dim. |
| C1F1.1 | 500x6 | 4 / 7x1 | - | - | 500x1 | 100 | - | 1 |
| C1F1.2 | 500x6 | 16 / 13x1 | - | - | 500x1 | 100 | - | 1 |
| C1F1.3 | 500x6 | 64 / 21x1 | - | - | 500x1 | 100 | - | 1 |
| C1F1.4 | 500x6 | 64 / 21x1 | - | - | 500x1 | 200 | - | 1 |
| C1F2 | 500x6 | 64 / 21x1 | - | - | 500x1 | 200 | 100 | 1 |
| CNN with multiple conv. layers | | | | | | | | |
| C2F1 | 500x6 | 4 / 7x1 | 16 / 13x1 | - | 500x1 | 100 | - | 1 |
| C3F1.1 | 500x6 | 4 / 7x1 | 16 / 13x1 | 64 / 21x1 | 500x1 | 100 | - | 1 |
| C3F1.2 | 500x6 | 4 / 7x1 | 16 / 13x1 | 64 / 21x1 | 500x1 | 200 | - | 1 |
| C3F2 | 500x6 | 4 / 7x1 | 16 / 13x1 | 64 / 21x1 | 500x1 | 200 | 100 | 1 |

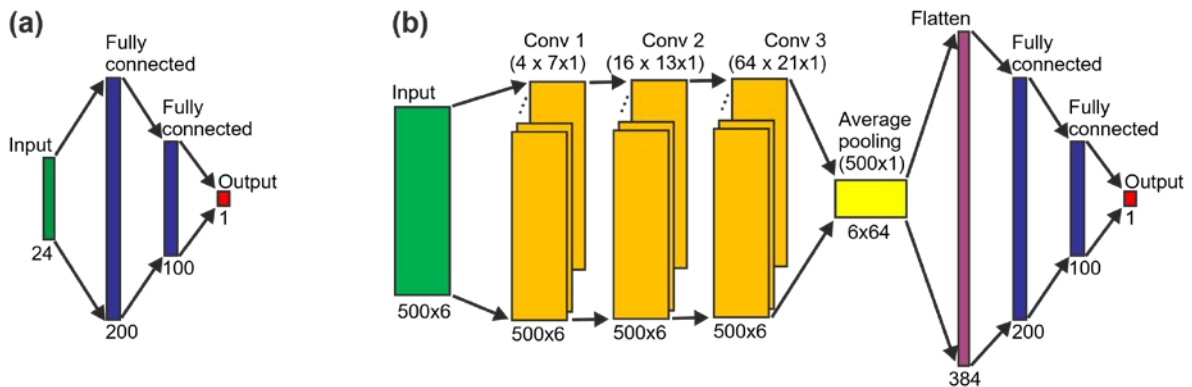


Figure 2: Schematic diagrams of the network architectures: **(a)** feed forward network F2, and **(b)** convolutional neural network C3F2. For more details, please see Table 1.

2.4 Evaluation Procedure and Quantification Measures

To evaluate and compare classification performance of the above presented neural network architectures, we used a 5-fold cross-validation procedure where we divided the dataset into five subsets (each subset contained samples from nine different infants) where each time one subset was used as a test set and the remaining four subsets were used to train the network architectures. The number of samples in the training and test sets for each fold is given in Table 2. In each fold in the training set, we had on average 662 (SD = 4) samples for the absent of figedy movements (FM-) and 758 (SD = 3) for the presence of figedy movements (FM+) class, and in the test set we had on average 166 (SD = 4) samples for the FM- and 190 (SD = 3) for the FM+ class.

The training set was split into training (5/6 of the training data) and validation (1/6 of the training data) subsets. For each fold we trained the network 20 times and then selected the model with the lowest loss score on the validation set which was evaluated on the test set.

For the evaluation of the classification performance, we use three common classification performance measures, i.e., sensitivity (true positive rate [TPR]), specificity (true negative rate [TNR]) and balanced accuracy (BA):

$$TPR = \frac{TP}{TP+FN}, TNR = \frac{TN}{TN+FP}, BA = \frac{TPR+TNR}{2},$$

where TP is the number of true positives, TN the number of true negatives, FP the number of false positives, and FN the number of false negatives.

Table 2: Data split of 5-fold cross-validation. The whole dataset contained 1776 samples (828 FM- and 948 FM+) obtained from 45 infants. Every fold contained samples from 36 and 9 infants for training set (~80% of samples) and test set (~20% of samples), respectively. Note that training set was split into training (83.33% [30 infants]) and validation (16.67% [6 infants]) subsets.

| Fold number | Training set (# of samples) | | | Test set (# of samples) | | |
|-------------|-----------------------------|-----|-------|-------------------------|-----|-------|
| | FM- | FM+ | Total | FM- | FM+ | Total |
| 1 | 662 | 761 | 1423 | 166 | 187 | 353 |
| 2 | 662 | 754 | 1416 | 166 | 194 | 360 |
| 3 | 665 | 760 | 1425 | 163 | 188 | 351 |
| 4 | 666 | 757 | 1423 | 162 | 191 | 353 |
| 5 | 657 | 760 | 1417 | 171 | 188 | 359 |

3. RESULTS

3.1 Signal Examples

Examples of pressure mat sensor values and extracted feature signals x , y , and p are shown in Fig. 3, where signals of one sample of FM- and one sample of FM+ are shown in panels (a1, b1) and (a2, b2), respectively. In panels (a1, a2) one can see a change of pressure activity patterns caused by the infant's movement. Extracted signals are shown in panels (b1, b2), where in case of no fidgety movements (FM-, [b1]) one can observe local (short) signal patterns of lower frequency but larger amplitude as compared to the FM+ case (b2), where local (short) signal patterns of higher frequency but larger amplitude can be observed which are presumably caused by infant's fidgety movements.

3.2 Classification Results

Results of classification performance for different neural architectures (see Table 1) are summarized and compared in Fig. 4 where all classification performance measures are provided in Table 3.

FFN architectures. In case of FFN architectures with manually defined statistical features, the worst classification performance on average was obtained when using only original signals x , y , and p (no derivatives, network F1.1) with average balanced accuracy $BA = 72.11\%$. Adding statistical features from signal derivatives x' , y' , and p' (network F1.3) and increasing the number of neurons in the fully connected layer from 100 to 200, improves classification performance (average $BA = 75.57\%$), however this improvement is not statistically significant (t -test, $p = 0.2080$). Adding a second fully connected layer (network F2) did not lead to better classification performance (average $BA = 73.58\%$).

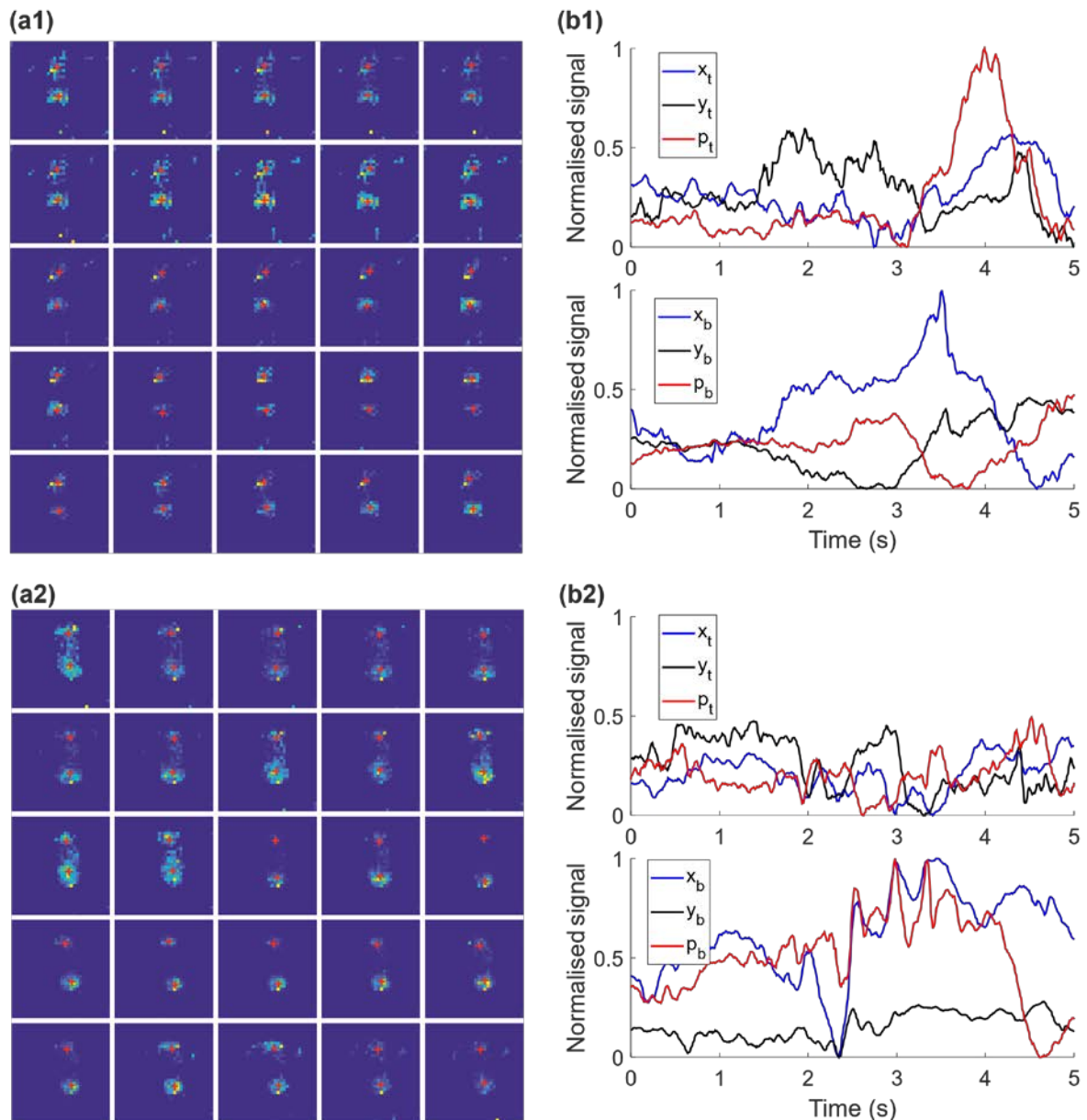


Figure 3: Examples of pressure mat values and extracted signals for one sample of the FM- (a1, b1) and one sample of the FM+ class (a2, b2). **(a)** Pressure mat values obtained at 0.2, 0.4, ..., 5s are shown where blue and red colours correspond to low- and high-pressure values, respectively. Red crosses correspond to the position of the centre of mass for the top and the bottom part of the pressure mat (see Fig. 1). **(b)** Signals for position x, y of the centre of mass, and average pressure p.

CNN architectures with a single convolutional layer. A CNN network architecture with learned features and only one convolutional layer (C1F1.1, four filters of size 7x1) leads to better classification performance on average as compared to the best FFN architecture, average BA is **77.46%** vs. 75.57%, however, this improvement is not statistically significant (*t-test*, $p=0.4305$).

Increasing the number of filters and the filter size (C1F1.2, 16 filters of size 13x1; C1F1.3, 64 filters of size 21x1) did not lead to better classification performance, average BA is 74.85% (C1F1.2) and 75.03% (C1F1.3). Increasing the number of neurons in the fully connected layer (C1F1.4) or adding a second fully connected layer (C1F2) did not improve classification performance either, average BA is 73.93% (C1F1.4) and 76.00% (C1F2).

CNN architectures with multiple convolutional layers. Using architectures with two (C2F1) or three convolutional layers (C3F.1-2, C3F2) further improved classification performance. The best classification performance was obtained by using a CNN architecture with three convolutional layers

and two fully connected layers (C3F2), average BA = **81.43%**. This architecture leads to statistically significant classification improvement by 5.85% (*t-test*, $p < 0.05$) as compared to the best FFN architecture (BA = 75.57%) with manually defined statistical features.

In summary, these results demonstrate that simple feed-forward network architectures (FFN) with manually defined statistical features can lead to a moderate classification accuracy (up to 75.6%). Furthermore, results show that using convolutional neural network architectures that allow learning relevant features instead of predefining them can lead to a better classification accuracy (up to 81.4%).

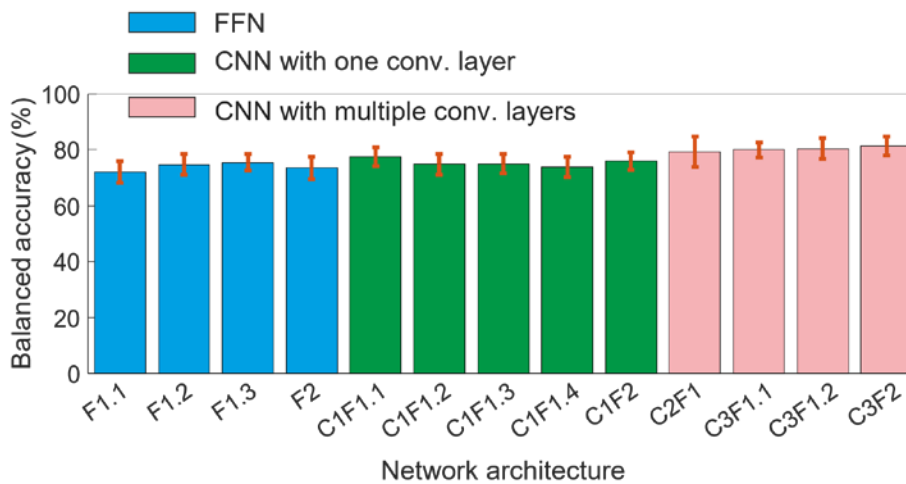


Figure 4: Comparison of different network architectures (see Table 1) on classification of fidgety movements. Average balanced accuracy is shown obtained on five test sets. Error bars denote confidence intervals of the mean (CI 95%).

Table 3: Comparison of different network architectures (see Table 1) on classification of fidgety movements. Average sensitivity, specificity and balanced accuracy is shown obtained on five test sets. Numbers in brackets correspond to confidence intervals of the mean (CI 95%).

| Name | Sensitivity (%) | Specificity (%) | Balanced Accuracy (%) |
|---------------------------------------|---------------------------|---------------------------|----------------------------------|
| FFN | | | |
| F1.1 | 73.9460 [70.6016 77.2905] | 70.2720 [59.1582 81.3857] | 72.1090 [68.1067 76.1112] |
| F1.2 | 81.3168 [78.4642 84.1693] | 68.2874 [60.8889 75.6858] | 74.8021 [71.1564 78.4477] |
| F1.3 | 79.9627 [77.1079 82.8175] | 71.1806 [63.4379 78.9234] | 75.5717 [72.6507 78.4927] |
| F2 | 79.8998 [74.0200 85.7795] | 67.2514 [54.6910 79.8119] | 73.5756 [69.5182 77.6330] |
| CNN with one conv. layer | | | |
| C1F1.1 | 85.3460 [82.4676 88.2244] | 69.5788 [62.0279 77.1296] | 77.4624 [74.0876 80.8372] |
| C1F1.2 | 81.6623 [76.6924 86.6322] | 68.0383 [58.1771 77.8995] | 74.8503 [71.1472 78.5534] |
| C1F1.3 | 80.5723 [78.1043 83.0402] | 69.4817 [64.0029 74.9604] | 75.0270 [71.5400 78.5139] |
| C1F1.4 | 78.0319 [74.1008 81.9630] | 69.8199 [62.5851 77.0546] | 73.9259 [70.3623 77.4895] |
| C1F2 | 79.2589 [75.6178 82.9001] | 72.7467 [65.0842 80.4092] | 76.0028 [72.9282 79.0774] |
| CNN with multiple conv. layers | | | |
| C2F1 | 84.4210 [80.1495 88.6925] | 74.2966 [62.4324 86.1607] | 79.3588 [73.8382 84.8794] |
| C3F1.1 | 84.4764 [79.2485 89.7043] | 75.7092 [68.6191 82.7994] | 80.0928 [77.3717 82.8139] |
| C3F1.2 | 86.0629 [81.8901 90.2358] | 74.8045 [67.7212 81.8878] | 80.4337 [76.6952 84.1722] |
| C3F2 | 86.4780 [82.9219 90.0340] | 76.3739 [70.7064 82.0414] | 81.4260 [77.9968 84.8551] |

4. DISCUSSION

Among different clinical diagnostic tools to examine the integrity of the developing nervous system, the Prechtl's general movements assessment has won out for its clinical significance and peerless efficiency [55]. Especially the outstanding predictive value of the presence/absence of age-specific

fidgety movements has gained extended attention both from clinicians and computer scientists. The latter have been developing automated approaches during the past decade aiming at future clinical implementation to complement man-powered classic GMA [7, 15]. While most approaches remain true to the GMA concept and work on vision-based algorithms, we proposed a multimodal approach to capture and analyse infant motion data [5]. In the current study, we carried out a proof-of-concept evaluation and explored the feasibility and potential of using a pressure sensing mat as an add-on to the vision-based methods to track and classify infant spontaneous movements. By empirically testing this method, we are able to compare its clinical value with other methods applying different kinds of motion sensors.

First, we compared the classification performance on *presence vs. absence* of the fidgety movements with the pressure sensing mat to the performances based on RGB or RGB-D videos in Table 4. Although video-based classification/recognition methods currently outperform (84-100%) the pressure-based classification, a high accuracy was achieved (81%) using the pressure data. Note that the mat used in this study was not specifically designed to measure infant motion. As technology advances continuously, more sensitive devices are likely to be available soon and more suitable for infant motion tracking, which may substantially improve the performance of the pressure-based classification. The lower performance can also be partially explained by the fact that the pressure sensing mat measures motion of body parts indirectly as compared to motion data obtained from full body tracking; i.e., infants often lift their legs and arms, thus, motion of extremities, which are in the air cannot be captured directly by the pressure sensing mat but are rather indirectly reflected by a change of pressure patterns. In addition, as mentioned in the Methods section, data used in the current study originated from a healthy, typically developing cohort. The absence of fidgety movements in this cohort reflects a normal, age-typical motor pattern, i.e., the writhing movements, which are known to have significantly different quality and motion appearance from the pathological motor patterns of absent fidgety movements [2]. Note that typically developing infants between 3 to 5 months of age do not demonstrate fidgety movements at all times, the predominant movement pattern counts [4, 31]. The pathological absence-of-fidgety patterns of infants with neurological deficits (e.g., with cramped-synchronised movement character; see [3]), when compared to normal fidgety movements of same aged infants, is likely to be easier to identify by the pressure mat, resulting in higher classification performance. Unfortunately, we do not have adequate data to prove this hypothesis for now. Future studies need to target extended datasets (as discussed below) to examine the performance of the pressure sensors. These studies should evaluate how motion sensors distinguish (a) normal absence of fidgety (i.e., age-typical writhing movements pattern without fidgety), (b) normal movement patterns during the fidgety age-period (from 9 weeks to about 20 weeks of post-term age), and (c) abnormal movement patterns (absent fidgety) during 9-20 weeks of post-term age. The current study tested the classification between (a) and (b). This, from the clinical perspective, is different than distinguishing between (b) and (c), which was the focus of most studies listed in Table 4. This might also explain their better performance. Further studies are warranted to compare the AI approaches within different tasks.

We also compared different sensor modalities for the acquisition of pose or motion information for automated infant movement assessment, focusing on their applicability and suitability in clinical settings (Table 5). Naturally, when working with young infants, external sensors are preferable since they are non-intrusive and do not require attaching sensors to the infant body. Sensor attachment may interfere with infant behavioural status and movements, which is against the principle of GMA [4]. Single RGB cameras are easy to install and operate (no synchronisation nor calibration required), yet these sensors provide only 2D pose/motion information as compared to accelerometer or inertial motion unit (IMU) sensors. In case of camera sensors, additional algorithms need to be applied to extract pose and/or motion information, whereas accelerometers, IMUs or a pressure sensing mat pro-

Table 4: Comparison of classification performance of different methods for recognition of fidgety movements.

| | Data | Classification/ Recognition | Classification performance measure | | | |
|--|----------------------|--------------------------------|------------------------------------|-----------|-----------------------|--------------|
| | | | Sens. (%) | Spec. (%) | Balanced accuracy (%) | Accuracy (%) |
| Current study | Pressure sensing mat | FM+ vs. FM- | 86 | 76 | 81 | |
| Reich et al., 2021 [31] | RGB video | FM+ vs. FM- | 88 | 88 | 88 | |
| McCay et al., 2021 [30] | RGB-D video* | FM+ vs. FM- | 100 | 100 | 100 | |
| Tsuji et al., 2020 [26] | RGB video | FM recognition | | | | 85 |
| Machireddy et al., 2017 [56] | RGB video | FM recognition | | | | 84 |
| Adde et al., 2013 [17] | RGB video | FM recognition | 89 | 79 | 84 | |
| Adde et al., 2009 [57] | RGB video | FM+ vs. FM- | 90 | 80 | 85 | |
| *Synthetic MINI-RGBD dataset generated from RGB-D videos [39]. | | | | | | |

vide motion information directly. Importantly, while the pressure sensing mat provides motion information in 3D space (2D position and pressure), this is quite different from the information obtained from video data (usually body pose) or inertial motion sensors (acceleration and/or angular velocity). Thus, pressure sensing mat data can augment other sensor modalities, especially single RGB or RGB-D camera setups to improve motion tracking. In addition, single RGB or RGB-D cameras frequently suffer from occlusions (either caused by the setup, e.g., in an incubator, or by the infant's motion) and may lose track of some body parts from time to time. This limitation may be solved by using multiple cameras. However, such a setup becomes notably more complicated due to the necessity for synchronisation and calibration of the cameras, and also due to the amount of information generated, which needs to be processed to obtain 3D body pose and/or motion information. By contrast, the fully non-intrusive pressure sensing mat is effortless to install and much more convenient to use, which has great potential for application with families with young infants in busy daily clinical routines.

In the clinical and research communities, the privacy of participants remains a high and sustaining concern [58]. With the pressure sensing data, individual identity protection is easily achieved since no personal identifiable data is necessary for the analyses. Different from this, with vision-based sensors (cameras), faces, being one of the most sensitive personal identifiers, are commonly recorded and present in the datasets. Data de-identification and privacy protection can only be done through additional technical manipulations. Thus, pressure sensing technologies are particularly favourable for easy large-scale multicentre data acquisition and sharing. Large datasets are essential for training machine learning algorithms and for evaluating and comparing performances of different AI approaches from different labs. Pressure sensing solutions, by nature pseudonymised, is thus a remarkably promising approach for worldwide efficient and convenient scientific and clinical applications. This is particularly helpful for data sharing between researchers and should greatly enhance collaboration.

Table 5: Comparison of different sensors for acquisition of pose or motion information.

| | Single RGB camera | Single RGB-D camera | Multiple RGB cameras | Multiple accelerometers/IMUs | Pressure sensing mat |
|--|--------------------------|--------------------------|--------------------------|---|--------------------------|
| Sensor type | External (non-intrusive) | External (non-intrusive) | External (non-intrusive) | Wearable (on-body) | External (non-intrusive) |
| Obtained pose/motion information | 2D pose | 3D pose | 3D pose | 3D acceleration and 3D angular velocity | 2D position and pressure |
| Extraction of pose/motion information | Indirect | Indirect | Indirect | Direct | Direct |
| Synchronisation required | NO | NO | YES | YES | NO |
| Calibration required | NO | NO | YES | YES | NO |
| Data privacy issue | YES | YES | YES | NO | NO |
| Applicability and handling in clinical settings | Easy | Easy | Complicated | Complicated | Easy |

5. CONCLUSION

In this study, we demonstrated that pressure sensing methodology can generate adequate infant movement classification for GMA. With ongoing technological advances on infant-suitable devices, easy-to-apply, non-intrusive pressure sensing solutions have great potential in daily clinical practice and surveillance of infant neuromotor functions. Developing pressure sensing approaches will forcefully contribute to meeting the urgent need of acquiring and sharing large datasets across centres. Our findings suggest that multimodal (e.g., pressure, accelerometry, vision) data acquisition and analyses is a promising approach, which combines different venues of motion information. This approach may optimise and streamline infant movement evaluations enabling efficient clinical implementation in the future.

ACKNOWLEDGEMENTS

The authors thank all families for their participation. Thanks to team members who were involved in recruitment, data acquisition, curation, and pre-processing: Magdalena Kriebler-Tomantschger, Iris Tomantschger, Laura Langmann, Claudia Zitta, Dr. Robert Peharz, Dr. Florian Pokorny, Dr. Simon Reich. We are/were supported by BioTechMed Graz and the Deutsche Forschungsgemeinschaft (DFG – stand-alone grant, SFB1528), the Laerdal Foundation, the Bill and Melinda Gates Foundation (OPP), the Volkswagenfoundation (project IDENTIFIED), the LeibnizScience Campus, the BMBF CP-Diadem Germany, and the Austrian Science Fund (KL1811) for data acquisition, preparation, and analyses. Special thanks also to our interdisciplinary international network of collaborators for discussing this study with us and for refining our ideas.

REFERENCES

- [1] C. Einspieler, D. Prayer, and P. B. Marschik, "Fetal movements: The origin of human behaviour," *Developmental Medicine & Child Neurology*, vol. 63, no. 10, pp. 1142–1148, 2021.
- [2] H. F. Prechtl, C. Einspieler, G. Cioni, A. F. Bos, F. Ferrari, and D. Sontheimer, "An early marker for neurological deficits after perinatal brain lesions," *The Lancet*, vol. 349, no. 9062, pp. 1361–1363, 1997.
- [3] C. Einspieler, P. B. Marschik, and H. F. Prechtl, "Human motor behavior: Prenatal origin and early postnatal development," *Zeitschrift für Psychologie/Journal of Psychology*, vol. 216, no. 3, p. 147, 2008.
- [4] C. Einspieler, H. Prechtl, A. Bos, F. Ferrari, and G. Cioni, *Prechtl's method on the qualitative assessment of general movements in preterm, term and young infants*. Mac Keith Press, 2004.
- [5] P. B. Marschik, F. B. Pokorny, R. Peharz, D. Zhang, J. O'Muircheartaigh, H. Roeyers, S. Bölte, A. J. Spittle, B. Urlsberger, B. Schuller *et al.*, "A novel way to measure and predict development: A heuristic approach to facilitate the early detection of neurodevelopmental disorders," *Current neurology and neuroscience reports*, vol. 17, no. 5, pp. 1–15, 2017.
- [6] I. Novak, C. Morgan, L. Adde, J. Blackman, R. N. Boyd, J. Brunstrom-Hernandez, G. Cioni, D. Damiano, J. Darrah, A.-C. Eliasson *et al.*, "Early, accurate diagnosis and early intervention in cerebral palsy: Advances in diagnosis and treatment," *JAMA pediatrics*, vol. 171, no. 9, pp. 897–907, 2017.
- [7] N. Silva, D. Zhang, T. Kulvicius, A. Gail, C. Barreiros, S. Lindstaedt, M. Kraft, S. Bölte, L. Poustka, K. Nielsen-Saines *et al.*, "The future of general movement assessment: The role of computer vision and machine learning—A scoping review," *Research in developmental disabilities*, vol. 110, p. 103854, 2021.
- [8] A. K.-L. Kwong, R. N. Boyd, M. D. Chatfield, R. S. Ware, P. B. Colditz, and J. M. George, "Early motor repertoire of very preterm infants and relationships with 2-year neurodevelopment," *Journal of clinical medicine*, vol. 11, no. 7, p. 1833, 2022.
- [9] C. Einspieler, A. F. Bos, M. E. Libertus, and P. B. Marschik, "The general movement assessment helps us to identify preterm infants at risk for cognitive dysfunction," *Frontiers in psychology*, vol. 7, p. 406, 2016.
- [10] C. Einspieler, R. Peharz, and P. B. Marschik, "Fidgety movements—tiny in appearance, but huge in impact," *Jornal de Pediatria*, vol. 92, pp. 64–70, 2016.
- [11] C. Peyton, C. Einspieler, T. Fjørtoft, L. Adde, M. D. Schreiber, A. Drobyshevsky, and J. D. Marks, "Correlates of normal and abnormal general movements in infancy and long-term neurodevelopment of preterm infants: Insights from functional connectivity studies at term equivalence," *Journal of clinical medicine*, vol. 9, no. 3, p. 834, 2020.
- [12] S. Salavati, C. Einspieler, G. Vagelli, D. Zhang, J. Pansy, J. G. Burgerhof, P. B. Marschik, and A. F. Bos, "The association between the early motor repertoire and language development in term children born after normal pregnancy," *Early Human Development*, vol. 111, pp. 30–35, 2017.
- [13] P. B. Marschik, W. E. Kaufmann, S. Bölte, J. Sigafos, and C. Einspieler, "En route to disentangle the impact and neurobiological substrates of early vocalizations: Learning from Rett syndrome," *Behav Brain Sci*, vol. 37, no. 6, pp. 562–3, 2014.
- [14] C. Einspieler and H. F. Prechtl, "Prechtl's assessment of general movements: A diagnostic tool for the functional assessment of the young nervous system," *Mental retardation and developmental disabilities research reviews*, vol. 11, no. 1, pp. 61–67, 2005.
- [15] M. T. Irshad, M. A. Nisar, P. Gouverneur, M. Rapp, and M. Grzegorzek, "AI approaches towards Prechtl's assessment of general movements: A systematic literature review," *Sensors*, vol. 20, no. 18, p. 5321, 2020.
- [16] L. Adde, J. L. Helbostad, A. R. Jensenius, G. Taraldsen, K. H. Grunewaldt, and R. Støen, "Early prediction of cerebral palsy by computer-based video analysis of general movements: A feasibility study," *Developmental Medicine & Child Neurology*, vol. 52, no. 8, pp. 773–778, 2010.
- [17] L. Adde, J. Helbostad, A. R. Jensenius, M. Langaas, and R. Støen, "Identification of fidgety movements and prediction of CP by the use of computer-based video analysis is more accurate when based on two video recordings," *Physiotherapy theory and practice*, vol. 29, no. 6, pp. 469–475, 2013.

- [18] L. Adde, H. Yang, R. Sæther, A. R. Jensenius, E. Ihlen, J.-y. Cao, and R. Støen, "Characteristics of general movements in preterm infants assessed by computer-based video analysis," *Physiotherapy Theory and Practice*, vol. 34, no. 4, pp. 286–292, 2018.
- [19] H. Rahmati, R. Dragon, O. M. Aamo, L. Adde, Ø. Stavadahl, and L. Van Gool, "Weakly supervised motion segmentation with particle matching," *Computer Vision and Image Understanding*, vol. 140, pp. 30–42, 2015.
- [20] H. Rahmati, H. Martens, O. M. Aamo, Ø. Stavadahl, R. Støen, and L. Adde, "Frequency analysis and feature reduction method for prediction of cerebral palsy in young infants," *IEEE Transactions on Neural Systems and Rehabilitation Engineering*, vol. 24, no. 11, pp. 1225–1234, 2016.
- [21] D. Das, K. Fry, and A. M. Howard, "Vision-based detection of simultaneous kicking for identifying movement characteristics of infants at-risk for neuro-disorders," in *2018 17th IEEE International Conference on Machine Learning and Applications (ICMLA)*. IEEE, 2018, pp. 1413–1418.
- [22] S. Orlandi, K. Raghuram, C. R. Smith, D. Mansueto, P. Church, V. Shah, M. Luther, and T. Chau, "Detection of atypical and typical infant movements using computer-based video analysis," in *2018 40th annual international conference of the IEEE engineering in medicine and biology society (EMBC)*. IEEE, 2018, pp. 3598–3601.
- [23] W. Baccinelli, M. Bulgheroni, V. Simonetti, F. Fulceri, A. Caruso, L. Gila, and M. L. Scattoni, "Movidia: A software package for automatic video analysis of movements in infants at risk for neurodevelopmental disorders," *Brain sciences*, vol. 10, no. 4, p. 203, 2020.
- [24] A. Caruso, L. Gila, F. Fulceri, T. Salvitti, M. Micai, W. Baccinelli, M. Bulgheroni, and M. L. Scattoni, "Early motor development predicts clinical outcomes of siblings at high-risk for autism: Insight from an innovative motion-tracking technology," *Brain Sciences*, vol. 10, no. 6, p. 379, 2020.
- [25] I. Doroniewicz, D. J. Ledwon, A. Affanasowicz, K. Kieszczynska, D. Latos, M. Matyja, A. W. Mitas, and A. Mysliwiec, "Writhing movement detection in newborns on the second and third day of life using pose-based feature machine learning classification," *Sensors*, vol. 20, no. 21, p. 5986, 2020.
- [26] T. Tsuji, S. Nakashima, H. Hayashi, Z. Soh, A. Furui, T. Shibasaki, K. Shima, and K. Shimatani, "Markerless measurement and evaluation of general movements in infants," *Scientific reports*, vol. 10, no. 1, pp. 1–13, 2020.
- [27] E. A. Ihlen, R. Støen, L. Boswell, R.-A. de Regnier, T. Fjørtoft, D. Gaebler-Spira, C. Labori, M. C. Loennecken, M. E. Msall, U. I. Möinichen *et al.*, "Machine learning of infant spontaneous movements for the early prediction of cerebral palsy: A multi-site cohort study," *Journal of clinical medicine*, vol. 9, no. 1, p. 5, 2020.
- [28] K. D. McCay, E. S. Ho, C. Marcroft, and N. D. Embleton, "Establishing pose based features using histograms for the detection of abnormal infant movements," in *2019 41st Annual International Conference of the IEEE Engineering in Medicine and Biology Society (EMBC)*. IEEE, 2019, pp. 5469–5472.
- [29] K. D. McCay, E. S. Ho, H. P. Shum, G. Fehringer, C. Marcroft, and N. D. Embleton, "Abnormal infant movements classification with deep learning on pose-based features," *IEEE Access*, vol. 8, pp. 51582–51592, 2020.
- [30] K. D. McCay, E. S. Ho, D. Sakkos, W. L. Woo, C. Marcroft, P. Dulson, and N. D. Embleton, "Towards explainable abnormal infant movements identification: A body-part based prediction and visualisation framework," in *2021 IEEE EMBS International Conference on Biomedical and Health Informatics (BHI)*. IEEE, 2021, pp. 1–4.
- [31] S. Reich, D. Zhang, T. Kulvicius, S. Bölte, K. Nielsen-Saines, F. B. Pokorny, R. Peharz, L. Poustka, F. Wörgötter, C. Einspieler *et al.*, "Novel AI driven approach to classify infant motor functions," *Scientific Reports*, vol. 11, no. 1, pp. 1–13, 2021.
- [32] B. Nguyen-Thai, V. Le, C. Morgan, N. Badawi, T. Tran, and S. Venkatesh, "A spatio-temporal attention-based model for infant movement assessment from videos," *IEEE Journal of Biomedical and Health Informatics*, vol. 25, no. 10, pp. 3911–3920, 2021.
- [33] K. Raghuram, S. Orlandi, P. Church, M. Luther, A. Kiss, and V. Shah, "Automated movement analysis to predict cerebral palsy in very preterm infants: An ambispective cohort study," *Children*, vol. 9, no. 6, p. 843, 2022.
- [34] D. Groos, L. Adde, S. Aubert, L. Boswell, R.-A. de Regnier, T. Fjørtoft, D. Gaebler-Spira, A. Haukeland, M. Loennecken, M. Msall, U. I. Möinichen, A. Pascal, C. Peyton, H. Ramampiaro, M. D.

Schreiber, I. E. Silberg, N. T. Songstad, N. Thomas, C. Van den Broeck, G. K. Øberg, E. A. Ihlen, and R. Støen, "Development and validation of a deep learning method to predict cerebral palsy from spontaneous movements in infants at high risk," *JAMA Network Open*, vol. 5, no. 7, pp. e2221325–e2221325, 07 2022.

[35] H. I. Shin, H.-I. Shin, M. S. Bang, D.-K. Kim, S. H. Shin, E.-K. Kim, Y.-J. Kim, E. S. Lee, S. G. Park, H. M. Ji *et al.*, "Deep learning-based quantitative analyses of spontaneous movements and their association with early neurological development in preterm infants," *Scientific Reports*, vol. 12, no. 1, pp. 1–9, 2022.

[36] M. M. Serrano, Y.-P. Chen, A. Howard, and P. A. Vela, "Lower limb pose estimation for monitoring the kicking patterns of infants," in *2016 38th Annual International Conference of the IEEE Engineering in Medicine and Biology Society (EMBC)*. IEEE, 2016, pp. 2157–2160.

[37] A. Cenci, D. Liciotti, E. Frontoni, P. Zingaretti, and V. P. Carnielli, "Movements analysis of preterm infants by using depth sensor," in *Proceedings of the 1st International Conference on Internet of Things and Machine Learning, 2017*, pp. 1–9.

[38] S. S. Shivakumar, H. Loeb, D. K. Bogen, F. Shofer, P. Bryant, L. Prosser, and M. J. Johnson, "Stereo 3d tracking of infants in natural play conditions," in *2017 International Conference on Rehabilitation Robotics (ICORR)*. IEEE, 2017, pp. 841–846.

[39] N. Hesse, C. Bodensteiner, M. Arens, U. G. Hofmann, R. Weinberger, and A. Sebastian Schroeder, "Computer vision for medical infant motion analysis: State of the art and RGB-D data set," in *Proceedings of the European Conference on Computer Vision (ECCV) Workshops*. Springer International Publishing, 2018, pp. 32–49.

[40] N. Hesse, S. Pujades, M. J. Black, M. Arens, U. G. Hofmann, and A. S. Schroeder, "Learning and tracking the 3d body shape of freely moving infants from RGB-D sequences," *IEEE transactions on pattern analysis and machine intelligence*, vol. 42, no. 10, pp. 2540–2551, 2019.

[41] S. Moccia, L. Migliorelli, R. Pietrini, and E. Frontoni, "Preterm infants' limb-pose estimation from depth images using convolutional neural networks," in *2019 IEEE Conference on Computational Intelligence in Bioinformatics and Computational Biology (CIBCB)*. IEEE, 2019, pp. 1–7.

[42] K. D. McCay, P. Hu, H. P. Shum, W. L. Woo, C. Marcroft, N. D. Embleton, A. Munteanu, and E. S. Ho, "A pose-based feature fusion and classification framework for the early prediction of cerebral palsy in infants," *IEEE Transactions on Neural Systems and Rehabilitation Engineering*, vol. 30, pp. 8–19, 2022.

[43] V. Marchi, V. Belmonti, F. Cecchi, M. Coluccini, P. Ghirri, A. Grassi, A. Sabatini, and A. Guzzetta, "Movement analysis in early infancy: Towards a motion biomarker of age," *Early Human Development*, vol. 142, p. 104942, 2020.

[44] H. U. Chung, A. Y. Rwei, A. Hourlier-Fargette, S. Xu, K. Lee, E. C. Dunne, Z. Xie, C. Liu, A. Carlini, D. H. Kim *et al.*, "Skin-interfaced biosensors for advanced wireless physiological monitoring in neonatal and pediatric intensive-care units," *Nature medicine*, vol. 26, no. 3, pp. 418–429, 2020.

[45] C. Fontana, V. Ottaviani, C. Veneroni, S. E. Sforza, N. Pesenti, F. Mosca, O. Picciolini, M. Fumagalli, and R. L. Dellacà, "An automated approach for general movement assessment: A pilot study," *Frontiers in pediatrics*, p. 868, 2021.

[46] M. S. Abrishami, L. Nocera, M. Mert, I. A. Trujillo-Priego, S. Purushotham, C. Shahabi, and B. A. Smith, "Identification of developmental delay in infants using wearable sensors: Full-day leg movement statistical feature analysis," *IEEE journal of translational engineering in health and medicine*, vol. 7, pp. 1–7, 2019.

[47] M. Airaksinen, O. Räsänen, E. Ilén, T. Häyrinen, A. Kivi, V. Marchi, A. Gallen, S. Blom, A. Varhe, N. Kaartinen *et al.*, "Automatic posture and movement tracking of infants with wearable movement sensors," *Scientific reports*, vol. 10, no. 1, pp. 1–13, 2020.

[48] D. den Hartog, M. M. van der Krogt, S. van der Burg, I. Aleo, J. Gijsbers, L. A. Bonouvrié, J. Harlaar, A. I. Buizer, and H. Haberfehlner, "Home-based measurements of dystonia in cerebral palsy using smartphone-coupled inertial sensor technology and machine learning: A proof-of-concept study," *Sensors*, vol. 22, no. 12, p. 4386, 2022.

- [49] D. Karch, K.-S. Kim, K. Wochner, J. Pietz, H. Dickhaus, and H. Philippi, "Quantification of the segmental kinematics of spontaneous infant movements," *Journal of biomechanics*, vol. 41, no. 13, pp. 2860–2867, 2008.
- [50] D. Karch, K. Wochner, K. Kim, H. Philippi, M. Hadders-Algra, J. Pietz, and H. Dickhaus, "Quantitative score for the evaluation of kinematic recordings in neuropsychiatric diagnostics," *Methods of information in medicine*, vol. 49, no. 05, pp. 526–530, 2010.
- [51] M. Kriber-Tomantschger, F. B. Pokorny, I. Kriber-Tomantschger, L. Langmann, L. Poustka, D. Zhang, S. Treue, N. K. Tanzer, C. Einspieler, P. B. Marschik *et al.*, "The development of visual attention in early infancy: Insights from a free-viewing paradigm," *Infancy*, vol. 27, no. 2, pp. 433–458, 2022.
- [52] "Tecscan," <https://www.tekscan.com/pressure-mapping-sensors>, accessed: 2022-07-15.
- [53] "Tensorflow," <https://www.tensorflow.org/>, accessed: 2022-07-15.
- [54] "Keras," <https://keras.io/>, accessed: 2022-07-15.
- [55] M. Bosanquet, L. Copeland, R. Ware, and R. Boyd, "A systematic review of tests to predict cerebral palsy in young children," *Developmental Medicine & Child Neurology*, vol. 55, no. 5, pp. 418–426, 2013.
- [56] A. Machireddy, J. Van Santen, J. L. Wilson, J. Myers, M. Hadders-Algra, and X. Song, "A video/IMU hybrid system for movement estimation in infants," in *2017 39th Annual International Conference of the IEEE Engineering in Medicine and Biology Society (EMBC)*. IEEE, 2017, pp. 730–733.
- [57] L. Adde, J. L. Helbostad, A. R. Jensenius, G. Taraldsen, and R. Støen, "Using computer-based video analysis in the study of fidgety movements," *Early human development*, vol. 85, no. 9, pp. 541–547, 2009.
- [58] G. Ursin, N. Malila, J. Chang-Claude, M. Gunter, R. Kaaks, E. Kampman, M. Lambe, F. van Leeuwen, P. Magnusson, M. C. Nilbert *et al.*, "Sharing data safely while preserving privacy," *The Lancet*, vol. 394, no. 10212, p. 1902, 2019.